

Fluid-driven resetting of titanite following ultrahigh-temperature metamorphism in southern Madagascar

Robert M. Holder^{a,b,*}, Bradley R. Hacker^a

^a Department of Earth Science, University of California, Santa Barbara, CA 93106, USA

^b Department of Earth and Planetary Sciences, Johns Hopkins University, Baltimore, MD 21218, USA

ARTICLE INFO

Editor: Balz K.

Keywords:

Titanite

U–Pb

Alteration

Recrystallization

Ultrahigh-temperature metamorphism

Madagascar

ABSTRACT

LA-ICP-MS U–Pb dates and EPMA trace-element maps of titanite were collected from calc-silicate gneisses of the Ikalamavony (peak T : 750–800 °C) and Anosy (peak T : 900–950 °C) domains in southern Madagascar to evaluate how titanite responds to high-temperature metamorphism, cooling, and retrogression. Fluid-mediated replacement of precursor titanite by titanite domains of different composition (interface-coupled dissolution-precipitation, ICDR) was the primary mechanism by which titanite was reset following high-grade metamorphism. Comparison of titanite U–Pb dates (530–490 Ma) with independent petrology and thermochronology indicates that the alteration occurred at temperatures as low as 300–500 °C. Apparent Zr temperatures (temperatures calculated assuming titanite–quartz–zircon equilibrium) in altered titanite are less than or equal to the metamorphic peak, but higher than the inferred alteration temperature, implying that Zr was removed, but that titanite–quartz–zircon equilibrium was not achieved during alteration. Although evidence for ICDR was observed in titanite samples separated by 10's to ~100 km, differences in U–Pb dates among samples, and even among titanite grains in the same thin section suggest that alteration at any given time was localized.

1. Introduction

Traditionally, titanite U–Pb dates have been interpreted as cooling ages corresponding to a temperature of ~600 °C (e.g. Cherniak, 1993; Mezger et al., 1991; Spear and Parrish, 1996; Tucker et al., 1987). However, more recent empirical studies—mostly using LA-ICP-MS, but also SIMS—have demonstrated that Pb diffusion in most natural titanite is negligible at $T < 850$ °C (e.g. Castelli and Rubatto, 2002; Gao et al., 2012; Garber et al., 2017; Kohn and Corrie, 2011; Kylander-Clark et al., 2008; Marsh and Smye, 2017; Spencer et al., 2013; Stearns et al., 2015, 2016; Walters and Kohn, 2017). In these empirical studies, neocrystallization, alteration/reaction with a fluid, or plastic deformation were interpreted to be the main mechanisms by which U–Pb dates and elemental compositions were reset in titanite. Alteration/reaction with a fluid is envisioned to take place by interface-coupled dissolution-precipitation reactions (ICDR), in which a precursor titanite is partially replaced by titanite of different composition (see Putnis, 2009, for general discussion of ICDR).

Resetting (or partial resetting) of U–Pb dates by ICDR is well documented in phosphates (especially in monazite, but also in xenotime and apatite; see review by Engi, 2017) and zircon (see review by Rubatto, 2017). Fluid-mediated resetting of titanite is less well

described. Corfu and Muir (1989) recognized that titanite associated with greenschist-facies assemblages within a hydrothermal Au–Mo deposit in the Hemlo–Huron greenstone belt, Canada, were 8 Myr younger than titanite outside the deposit. Corfu (1996) found that titanite grains from samples separated by as little as 20 m in the Winnipeg River Subprovince, Canada, yield different dates; Corfu interpreted this to reflect “focused fluid activity”. Castelli and Rubatto (2002) argued that complex titanite zoning from marbles in the Sesia Zone of the Western Alps could not be explained by Pb diffusion, new titanite growth, or “a simple recrystallization process”; they concluded that the titanite grains experienced a “partial reequilibration process”. “Patchy” or lobate zoning in titanite—commonly inferred to be indicative of ICDR in other minerals—has long been recognized (e.g. Castelli and Rubatto, 2002; Franz and Spear, 1985; Rubatto and Hermann, 2001), but has only recently been explicitly interpreted as the result of ICDR (Bonamici et al., 2015; Garber et al., 2017; Marsh and Smye, 2017; Walters and Kohn, 2017). If ICDR is as important a process for resetting titanite U–Pb dates as these recent studies suggest, several questions need to be answered for the accurate interpretation of U–Pb titanite dates and Zr temperatures. Over what range of temperatures is titanite likely to react with a fluid? Can, for example, titanite react at temperatures as low as 100 °C, as suggested for zircon (Spandler et al., 2004)? Is radiogenic Pb

* Corresponding author at: Department of Earth Science, University of California, Santa Barbara, CA 93106, USA.

E-mail addresses: holder@jhu.edu (R.M. Holder), hacker@ucsb.edu (B.R. Hacker).

<https://doi.org/10.1016/j.chemgeo.2018.11.017>

Received 3 August 2018; Received in revised form 21 November 2018; Accepted 22 November 2018

Available online 08 December 2018

0009-2541/ © 2018 Elsevier B.V. All rights reserved.

efficiently removed from titanite during ICDR such that U-Pb dates acquired from replacement titanite record when ICDR occurred? To what extent is compositional equilibrium between titanite and other minerals in a rock—most importantly titanite–zircon–quartz equilibrium for Zr thermobarometry—achieved or maintained during ICDR? This study presents U-Pb dates, Zr thermobarometry, and major- and trace-element maps of titanite from high-temperature (HT) to ultrahigh-temperature (UHT) calc-silicate gneisses of southern Madagascar to evaluate how titanite responds to high-temperature metamorphism, cooling, and retrogression, with a focus on ICDR as a mechanism for resetting titanite U-Pb dates and Zr temperatures.

2. Studied samples and their geologic setting

Titanite from eight calc-silicate gneisses of the UHT Anosyen domain and one calc-silicate from the HT Ikalamavony domain (sample

12D2) were analyzed (Fig. 1). Complete sample descriptions are provided in Appendix A.1. Abbreviated sample descriptions are provided here and in Table 1.

Regionally extensive calc-silicate gneisses of the Anosyen domain (called the “Tranomaro Group” in GAF-BGR, 2008a) are characterized by the mineral assemblage scapolite + clinopyroxene + titanite ± quartz ± alkali feldspar ± plagioclase ± wollastonite ± calcite ± epidote ± fluorite ± spinel ± corundum ± hibonite. Trace amounts of zircon are present in all quartz-bearing samples. Baddelyite has been reported as a common accessory phase in quartz-absent calc-silicates near Tranomaro (Rakotondrazafy et al., 1996), but was not observed in the quartz-absent samples of this study. The sample from the Ikalamavony domain (12D2) contains Ca-amphibole, a mineral not observed in the studied calc-silicates from the Anosyen domain, consistent with the lower peak metamorphic temperatures in the Ikalamavony domain (e.g. GAF-BGR, 2008a; GAF-BGR, 2008b).

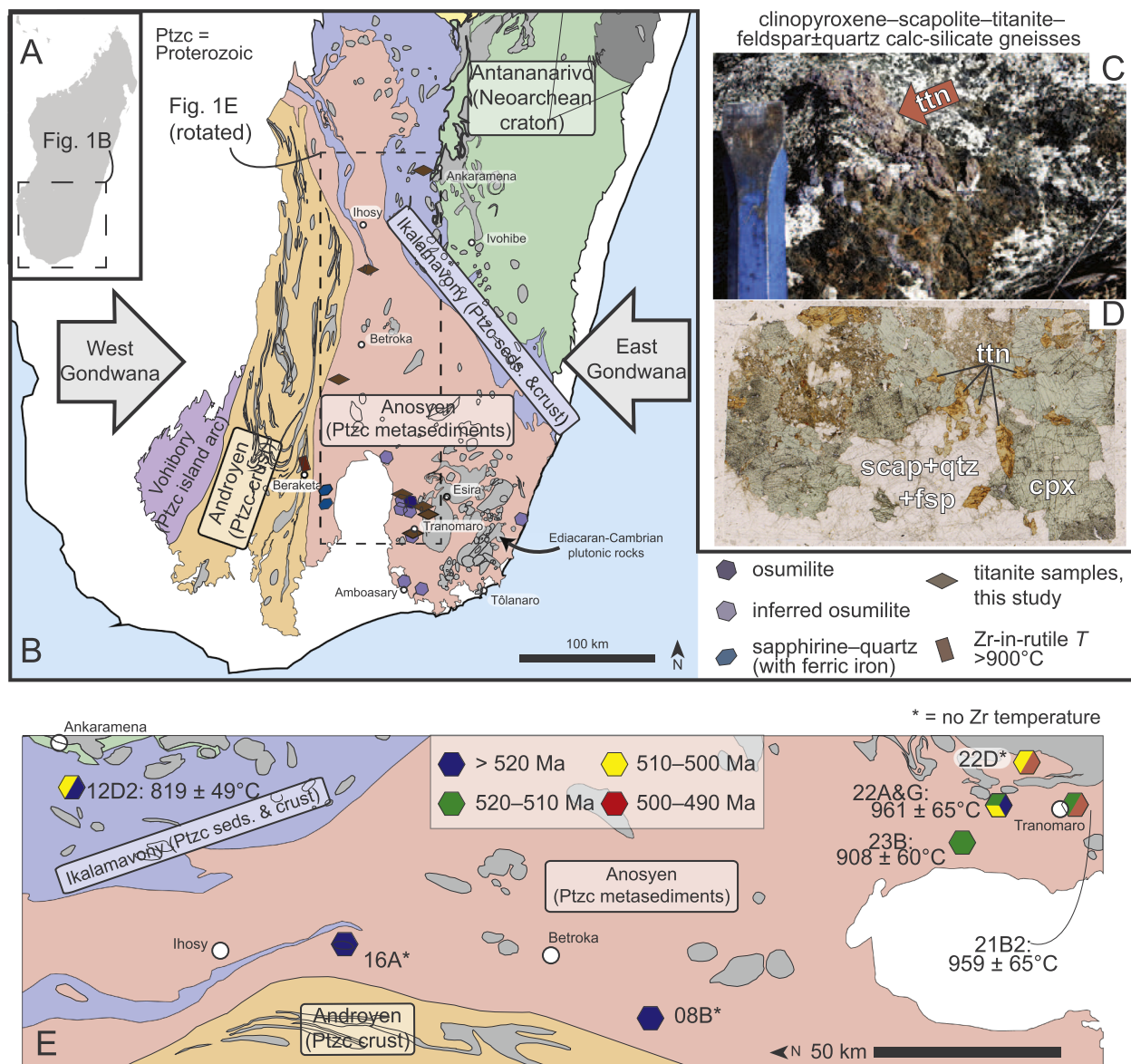


Fig. 1. (A) Location of study area in Madagascar. (B) Simplified geologic map of the tectonometamorphic domains of south Madagascar including the locations of diagnostic high-grade mineral assemblages (spinel–quartz is also ubiquitous in the Anosyen and eastern Androyen domains; modified from GAF-BGR, 2008a). (C) Typical outcrop of calc-silicate gneiss with large titanite: 2 cm chisel for scale. (D) Typical calc-silicate gneiss in thin section (2 × 4.5 cm), showing coarse-grain texture and lack of prominent foliation. (E) Enlarged geological map from B showing sample locations, U-Pb dates, and highest Zr temperatures. In samples without quartz (indicated by *), Zr temperatures are not shown, because the propagated uncertainty in the activity of SiO₂ is too large to be geologically useful (> ± 100 °C).

Table 1
Mineral assemblages and summary of U–Pb dates from each sample.

Tectonic domain	Sample ID	Short description	Major phases (> 5 vol%)	Minor phases (< 5 vol%)	U–Pb titanite dates	U–Pb monazite dates	Figure	
Anosyen	08B	Massive calc-silicate	Clinopyroxene, scapolite, titanite		524 ± 2.8 Ma ¹	–	S1	
	16A	Calc-silicate gneiss	Clinopyroxene, scapolite, titanite	Plagioclase, calcite	526.5 ± 2.3 Ma ¹	–	S1	
	21B2	Calc-silicate gneiss	Clinopyroxene, titanite, quartz, plagioclase, alkali-feldspar	Epidote	~520 to 490 Ma (see Figs. 3, 4 for details)	–	3, 4	
	22A	Massive calc-silicate	Clinopyroxene, scapolite, titanite, quartz, plagioclase		~525 to 505 Ma (see Fig. 5 for details)	–	5	
	22A4	Massive titanite boulder	Titanite	Alkali-feldspar, quartz	521.6 ± 3.6 Ma ¹	–	S1	
	22D	Massive calc-silicate	Clinopyroxene, scapolite, titanite	Corundum, spinel, fluorite, hibonite, calcite	525 ± 11 to 482 ± 11 Ma ²	–	7	
	22G	Massive calc-silicate	Clinopyroxene, scapolite, titanite, alkali-feldspar	Epidote, calcite	535 ± 17 to 495 ± 10 Ma ²	–	8	
	23B	Calc-silicate gneiss	Clinopyroxene, scapolite, titanite, epidote, plagioclase, alkali-feldspar, quartz		519.0 ± 2.4 Ma (unaltered) ¹ ; 488 ± 13 Ma (altered; one spot)	–	6	
	Ikkalamavony	04A1, -A2	Felsic gneiss	Garnet, biotite, quartz, plagioclase	Ilmenite	–	556 to 526 ± 13 Ma (-A1) ² ; 542.2 ± 4.8 & 1961 ± 26 Ma (-A2) ³	9
		04B1, -B2	Pelitic gneiss	Garnet, cordierite, biotite, sillimanite	Al-spinel	–	539.8 ± 1.9 Ma ¹	9
12D2		Calc-silicate gneiss	Clinopyroxene, plagioclase, scapolite, quartz, Ca-amphibole, titanite	Calcite, epidote, garnet, magnetite	537.1 ± 2.6 Ma (unaltered) ¹ ; 504.8 ± 2.5 Ma (altered) ¹	–	2	
12G		Pelitic gneiss lens in leucogneiss	Garnet, biotite, sillimanite, plagioclase, alkali-feldspar, quartz	Magnetite, ilmenite, Zn-rich Al-spinel	–	542.0 ± 3.4 Ma (in matrix) ¹ ; 573 to 531 ± 12 Ma (inclusions in garnet) ²	9	

¹ All dates are the at 95% confidence; date shown is the weighted mean ± 2se.

² Dates are not all the same at 95% confidence. Dates shown are the oldest and youngest spot analyses ± analytical uncertainty (2sd).

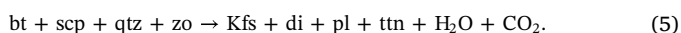
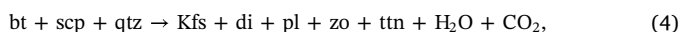
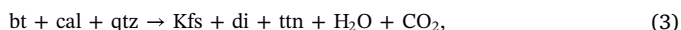
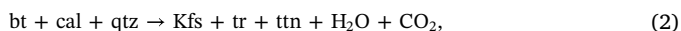
³ All analyses populate a discordia between a single inherited/detrital date and a metamorphic date. Dates shown are intercepts ± 2se.

Marbles, pyroxenites, and skarns associated with calc-silicate gneisses near Tranomaro, in the Anosyen domain, have been studied extensively as locations of sapphire, phlogopite, and U-Th mineralization resulting from *syn-* to post-metamorphic metasomatism (Boulvais et al., 1998, 2000; Martin et al., 2014; Moine et al., 1998; Pili et al., 1997a, 1997b; Rakotondrazafy et al., 1996; Ramambazafy et al., 1998). The samples presented in this study are not the mineralized rocks referenced in those works, with the possible exception of sample 22D, which contains corundum, hibonite, and fluorite. The rocks of this study are calc-silicate gneisses interpreted to be regionally metamorphosed “marls,” although, as discussed below, titanite dates and compositional zoning suggest that even these non-mineralized gneisses experienced at least a small degree of metasomatism perhaps related to the mineralization.

The generally well-equilibrated textures of the samples and lack of diagnostic inclusions in titanite mean that it is not possible to infer the metamorphic reactions that resulted in titanite growth in the samples of this study (e.g. Fig. 1D). Titanite is commonly considered to form in calc-silicates during prograde metamorphism by the decarbonation reaction (Frost et al., 2000; Kohn, 2017; mineral abbreviations after Kretz, 1983):



Reactions with Ti-rich biotite as a reactant might also have been important for titanite formation during prograde metamorphism (Rapa et al., 2017):



In each of reactions (1)–(5), titanite is the high-temperature Ti-bearing phase. In general, titanite is the stable Ti-phase (over rutile and ilmenite) at high-*T* in calc-silicates (e.g. Frost et al., 2000; Kohn, 2017; Rapa et al., 2017). In sample 22D, hibonite formation might have involved titanite breakdown, as indicated by the hibonite's relatively high Ti and REE concentrations (Rakotondrazafy et al., 1996; precise reactions not determined).

The metamorphic history of the Anosyen domain has been extensively evaluated by several recent studies (Boger et al., 2012; Holder et al., 2018a, 2018b; Horton et al., 2016; Jöns and Schenk, 2011); the results of these studies are summarized here. The domain is inferred to have been metamorphosed between 580 and 500 Ma along a clockwise *P–T* path in response to continental collision between the Dharwar and Congo cratons at the end of the East-African Orogeny. The peak temperature reached prior to decompression and cooling is inferred to have been 900–1000 °C and occurred between 560 and 540 Ma. The pressure of metamorphism at peak temperature, prior to decompression and cooling, was 0.5–1.0 GPa. The cooling history of the domain is best constrained by (thermo)chronology at Manangotry Pass (Montel et al., 2018): 540–530 Ma U/Th–Pb monazite dates from 750 to 800 °C biotite–apatite veins, 530–510 Ma U/Th–He dates from cm-scale monazite (300–400 °C), and a 455 ± 6 Ma biotite $^{40}\text{Ar}/^{39}\text{Ar}$ date (~300 °C). Titanite petrochronology from the Anosyen domain in this study is interpreted in the context of this independently constrained thermal history.

The metamorphic history of the Ikalamavony domain has been less extensively studied than the metamorphic history of the Anosyen domain. To provide additional constraints on the (*P–T*)–*t* history of the Ikalamavony domain for more rigorous interpretation of the titanite petrochronology, three felsic–pelitic gneisses, collected between Ankaramena and Ihozy, were also studied. The mineral assemblages of these samples are listed in Table 1. Complete sample descriptions are

given in Appendix A.1. Monazite U–Pb dates were collected from all three felsic–pelitic samples. *P–T* estimates were calculated using traditional thermobarometry of pelitic sample 12G (Section 3.5) and Zr-in titanite thermobarometry of calc-silicate sample 12D2 (section 3.4). The metamorphic history of the Ikalamavony domain is discussed in more detail in sections 4.3 and 5.2.

3. Methods

3.1. Laser-ablation split-stream inductively coupled plasma mass spectrometry (LASS)

U–Pb dates and trace-element composition of titanite were measured by LASS (Kylander-Clark et al., 2013; Kylander-Clark, 2017) at the University of California, Santa Barbara. Data are presented in Table A.1. U, Th, and Pb were measured on a Nu Plasma HR ICP-MS. All other elements were measured on an Agilent 7700 × ICPMS. The spot diameter was 40 μm and the laser fluence 2.4 J/cm². Each analysis was measured by firing the laser at 4 Hz for 20 s. U–Pb dates were corrected for down-hole fractionation, mass bias, and machine drift using Iolite (“U–Pb Geochronology 3” data reduction scheme; Paton et al., 2011) version 2.5 with Bear Lake Ridge titanite as the primary reference material (“BLR”; Aleinikoff et al., 2007). Secondary titanite reference materials Y1710C5 titanite (Spencer et al., 2013) and C513 titanite (in-house, c. 105 Ma) were used to check U–Pb date accuracy. The titanite dates in this study should be considered accurate to ± 2% when comparing to dates of other studies (Spencer et al., 2013). Because the secondary titanite reference materials are not isotopically homogeneous, a homogeneous zircon reference material (“Sri Lanka Zircon”; Gehrels et al., 2008) was used to assess data precision; following data processing in Iolite, an additional 2% uncertainty was propagated in quadrature to the $^{238}\text{U}/^{206}\text{Pb}$ and $^{207}\text{Pb}/^{206}\text{Pb}$ ratios of each analysis so that all analyses from the zircon (*n* = 20) were a single-population by the MSWD criterion (Wendt and Carl, 1991). Secondary reference material U–Pb measurements are presented in Table A.2. Elemental concentrations were calculated using the “Trace Elements” data reduction scheme of Iolite, assuming 19.25 wt% Ca in each unknown titanite analysis and using BHVO2G glass (GEOREM database preferred values) as the primary reference material.

LASS monazite dates were also collected from felsic–pelitic gneisses of the Ikalamavony domain between Ankaramena and Ihozy for comparison with titanite dates in sample 12D2 and to better constrain the timing of metamorphism. Monazite dates of this study were collected during the same analytical sessions as monazite dates presented by Holder et al. (2018a; see their supplementary information for analytical details and reference-material reproducibilities). Data are presented in Table A.3. A single, large monazite from Manangotry Pass was also dated; it yielded a concordant, single-population U/Th–Pb age of 570 ± 11 Ma (Fig. A.1), the oldest monazite date yet reported from this well-characterized locality (Montel et al., 2018, and references therein).

3.2. Trace-element maps and back-scattered electron images

Al, Fe, Zr, Nb, and Ce were mapped using a Cameca SX100 EPMA at the University of California, Santa Barbara. The maps were collected using a 1 μm pixel size and 1 s dwell time per pixel. Beam current was 200 nA. Accelerating voltage was 15 kV. The diameter of the activation volume (the volume from which 95% of X-rays were generated) at these beam conditions was estimated to have been ~1.5 μm using the program CASINO version 2.4.8.1, slightly larger than the pixel size used during data collection. The Zr and Nb *L_α* x-rays were measured using an LPET crystal; Al *K_α* using a TAP; Fe *K_α* and Ce *L_α* using an LLIF. Maps were collected using Probe Image and processed further using Calc Image of the Probe for EPMA software. Back-scattered electron images

were collected using an FEI Quanta 400f field-emission scanning-electron microscope, also at the University of California, Santa Barbara. BSE images were used as a guide for placement of the LA-ICP-MS analyses; in particular, μm -scale BSE-bright inclusions of zircon were identified in some altered titanite grains and avoided during LA-ICP-MS analysis.

3.3. Mineral compositions for thermobarometry

Major-element concentrations in pelitic gneiss sample 12G of the Iklamavony domain were measured using a Cameca SX100 EPMA at the University of California, Santa Barbara. Beam current was 10 nA.

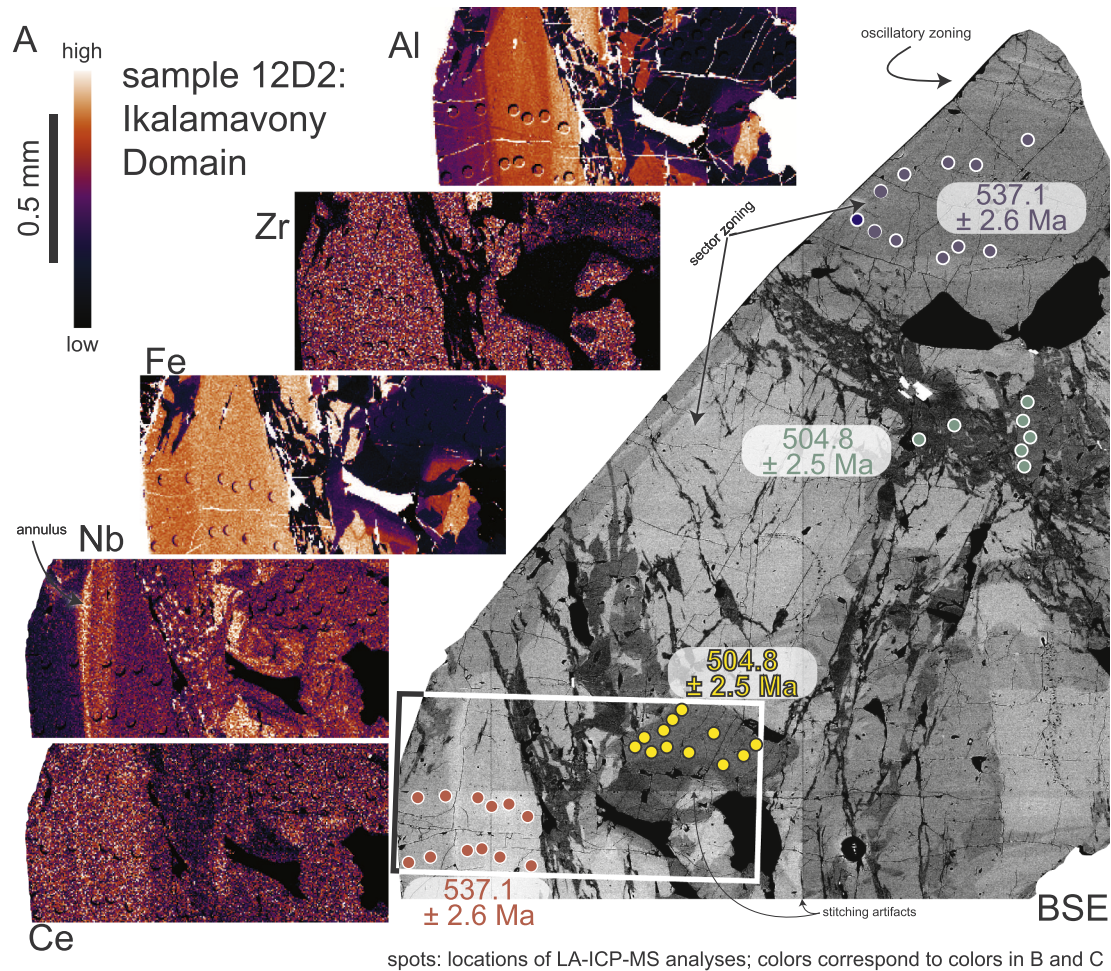


Fig. 2. Titanite data from sample 12D2 from the Ikalamavony domain. (A) EPMA x-ray maps of trace elements and back-scattered-electron (BSE) image of large titanite from sample 12D. Oscillatory and sector zoning along with annuli parallel to the crystal faces reflect compositional variation during growth of the grain. Alteration along fractures resulted in changes in composition and resetting of U-Pb dates. (B) U-Pb dates from unaltered titanite (blue and red spots in A) are all the same within uncertainty— 537.2 ± 2.6 Ma—and there is no resolvable relationship between date and distance from grain rim indicating that—at the scale of observation—volume diffusion of Pb did not modified the U/Pb ratio after titanite growth. Altered titanite (yellow and green spots in A) yields a consistent date of 504.8 ± 2.6 Ma. (C) The growth temperature of the grain (taken as the sector zone with the lower Zr concentrations; see [Kohn, 2017](#)) was 812 ± 49 $^{\circ}\text{C}$. Although altered titanite yields a consistent U-Pb date, Zr concentrations are heterogeneous suggesting that Zr was not as efficiently mobilized as Pb during alteration. (For interpretation of the references to colour in this figure legend, the reader is referred to the web version of this article.)

Accelerating voltage was 15 kV. $K\alpha$ x-rays were measured using the following crystals: LPET for K and Ca; TAP for Si and Al; LTAP for Na and Mg; LLIF for Ti, Mn, Fe, Zn, and Cr. Data were collected on-peak for 20 s. A mean-atomic-number background correction was used (Donovan et al., 2016). Data were collected and processed using the Probe for EPMA software. Data are presented in Table A.4.

3.4. Zr-in-titanite thermobarometry

Zr-in-titanite temperatures were calculated for each sample using the experimental calibration of Hayden et al. (2008). Quoted temperatures were calculated assuming a metamorphic pressure of 0.6 GPa. Reported uncertainties are the propagated 2σ uncertainties of the coefficients of the experimental calibration, Zr measurements, pressure (taken as ± 0.2 GPa), and a_{TiO_2} . For a_{TiO_2} , a value of 0.75 with a conservatively large uncertainty of ± 0.25 was used, reflecting the absence of rutile in the samples ($a_{\text{TiO}_2} < 1$), but that a_{TiO_2} is likely > 0.5 in titanite-bearing rocks (Chambers and Kohn, 2012; Ghent and Stout, 1984). Zr temperatures were not calculated in samples lacking quartz, because neither zircon nor baddeleyite was observed in thin section and the propagated uncertainties in a_{SiO_2} (as low as 0.1 in the corundum–hibonite calc-silicates; Rakotonirafy et al., 1996) in addition to the other uncertainties mentioned above, result in temperature uncertainties too large to be geologically useful ($> \pm 100$ °C). Data are presented in Table A.1.

3.5. Traditional thermobarometry of sample 12G

P – T conditions of metamorphism in the Ikalamavony domain were also calculated from the compositions of plagioclase, biotite, and garnet in equilibrium with sillimanite and quartz in sample 12G using the avPT mode of THERMOCALC (Powell and Holland, 1994). Mineral end-member thermodynamic data were taken from Holland and Powell (2011).

4. Results

Titanite dates reported in this section are $^{238}\text{U}/^{206}\text{Pb}$ dates corrected for initial Pb (Pb incorporated into titanite during growth) using $^{207}\text{Pb}/^{206}\text{Pb}_{\text{clinopyroxene}}$, because clinopyroxene in these rocks has no measurable U (using the same LASS analytical conditions as for titanite). Samples that exhibit a range of initial titanite Pb concentrations (variable $^{207}\text{Pb}/^{206}\text{Pb}_{\text{titanite}}$) are fit well by Tera-Wasserburg discordia anchored to $^{238}\text{U}/^{206}\text{Pb} = 0$ and $^{207}\text{Pb}/^{206}\text{Pb} = ^{207}\text{Pb}/^{206}\text{Pb}_{\text{clinopyroxene}}$ (samples 21B2 grain 1, 22A grain2, 08B, and 16A), suggesting that this initial-Pb correction is accurate, at least in those samples. However, the isotopic composition of Pb incorporated into titanite can be more radiogenic than that of the bulk rock if the titanite formed at the expense of a high- μ phase such as rutile (Kirkland et al., 2017, 2018; Marsh and Smye, 2017; Romer and Rötzler, 2003). If this were true for any of the Madagascar calc-silicates, the dates and inferred alteration temperatures reported herein are maxima. Values of $^{207}\text{Pb}/^{206}\text{Pb}_{\text{clinopyroxene}}$ in each sample are presented in Table A.5.

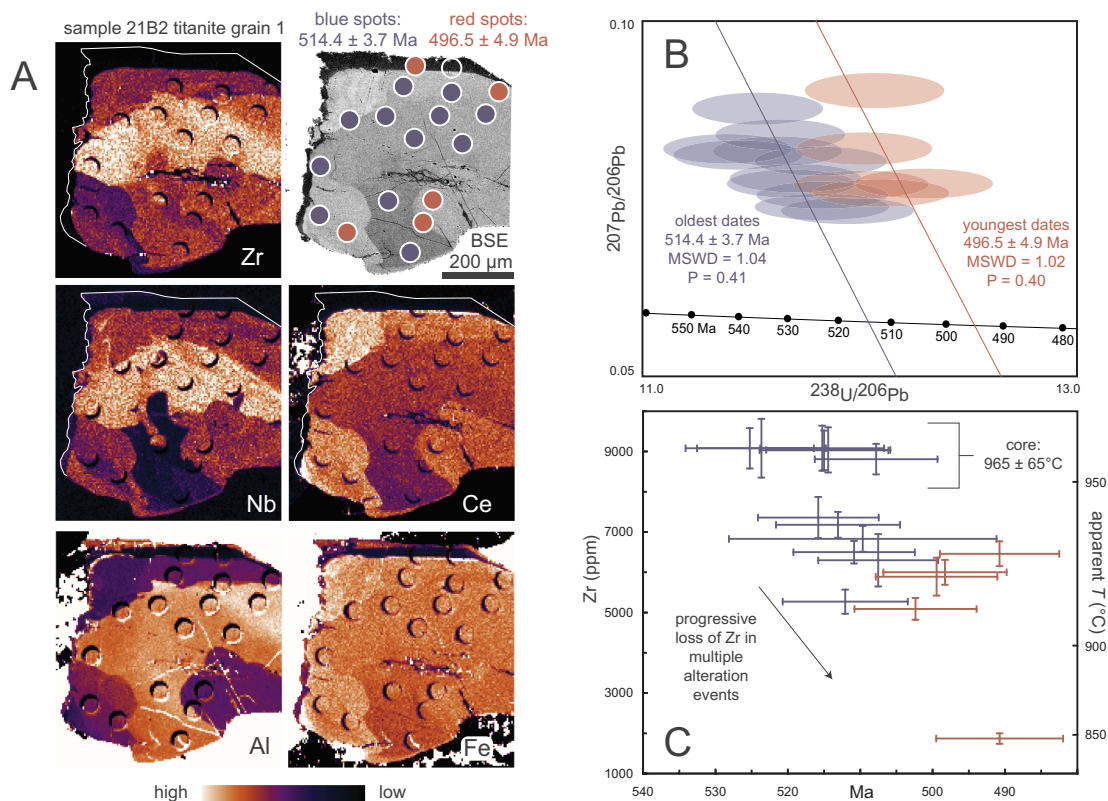


Fig. 3. Titanite data from sample 21B2 grain 1 from the Anosyen domain. (A) EPMA x-ray maps of trace elements and back-scattered-electron image of sample 21B2 titanite grain 1. The grain exhibits lobate domains of distinct composition with convex shapes toward the center of the grain. The lobate domains are interpreted to be the result of reaction with a fluid, specifically interface-coupled dissolution-precipitation (Putnis, 2009) in which precursor titanite is replaced by titanite of difference composition, as suggested by Garber et al. (2017) and Marsh and Smye (2017) for titanite in granitic and mafic rocks, respectively. (B) The oldest U-Pb dates are 514 Ma and the youngest dates are 497 Ma. There is no clear core-to-rim gradient in U-Pb dates, indicating that the range in dates is not the result of Pb loss by volume diffusion. (C) The core of the grain yields an apparent Zr temperature of 965 ± 65 °C, consistent with independent estimates for peak metamorphism which occurred at ~ 550 Ma (Holder et al., 2018a). Preservation of peak- T Zr concentrations during low- T alteration (U/Th–He monazite dates of 530–510 Ma indicate $T \leq 400$ °C at this time; Montel et al., 2018), suggest that titanite–quartz–zircon equilibrium was not maintained during resetting of U-Pb dates.

Individual spot analyses reported in this section have a 2σ precision of $\sim \pm 2\%$ based on secondary-reference-material reproducibility during the analytical session: $\sim \pm 10$ Myr. Groups of analyses that are statistically homogeneous by the MSWD criterion at the 95% confidence interval (Wendt and Carl, 1991) are reported as weighted means with 2-standard-error-of-the-mean (2se) uncertainties. The 2se uncertainties of weighted means are often $< 1\%$ of the mean (± 2 –4 Myr) and should be used only for comparing titanite dates within this study. For comparing dates of this study (individual spots or weighted means) with dates of other studies, the full accuracy of LA-ICP-MS titanite dates must be considered; Spencer et al. (2013) estimated this to be $\pm 2\%$ of the measured date, or $\sim \pm 10$ Myr.

4.1. Titanite petrochronology

Data from sample 12D2 of the Iklamavony domain are presented in Fig. 2. Titanite from this sample is characterized by oscillatory and sector zoning interpreted to reflect compositional variation during growth. Growth zoning is cut by patchy, lobate domains of distinct composition following fractures; these domains are interpreted to be the result of ICDR and are hereafter referred to as “altered” titanite. U-Pb dates from unaltered titanite (blue and red spots in Fig. 2A) are all the same: 537.1 ± 2.6 Ma. There is no resolvable relationship between date and distance from grain rim, suggesting that Pb diffusion was too slow and/or that the cooling rate was too fast to result in resolvable differences in U-Pb date with the $\sim \pm 2\%$ analytical precision of LASS. The Zr-in-titanite temperature of the unaltered part of the grain was 812 ± 49 °C (specifically the sector zone with less Zr, which is more likely to represent the growth temperature; see Hayden et al., 2008). U-

Pb dates from altered titanite (yellow and green spots in Fig. 2A) are homogeneous, but younger than dates from unaltered titanite: 504.8 ± 2.5 Ma. Although altered titanite yields a homogeneous U-Pb date, Zr concentrations are heterogeneous, corresponding to apparent temperatures of 650–800 °C.

U-Pb dates from samples within the Anosyen domain are summarized here and presented sample-by-sample in the following paragraphs. U-Pb dates from range from 530 to 490 Ma; there is no resolvable relationship between U-Pb date and distance from grain rims suggesting that Pb diffusion was too slow and/or that the cooling rate was too fast to result in resolvable differences in U-Pb date. This is consistent with 530–510 Ma monazite U/Th-He dates from Manangotry pass which indicate that the Anosyen domain had cooled to ≤ 400 °C by this time (Montel et al., 2018). Even the fastest estimates for Pb volume diffusion in crystalline titanite suggest the length-scales of diffusion should be negligible at $T < 600$ °C (Cherniak, 1993). Differences in U-Pb dates within individual grains are observed among “patchy” or lobate compositional domains, which extend into titanite from fractures and grain boundaries. These are interpreted to be the result of ICDR. In some grains, several generations of ICDR were observed in individual grains as differences in BSE intensity or chemical composition, although the age differences among the domains are not always resolvable.

Data from sample 21B2 of the Anosyen domain are presented in Figs. 3 and 4. Two grains were studied in detail. Grain 1 (Fig. 3) exhibits ≥ 3 cross-cutting lobate domains of distinct composition that extend toward the center of the grain; these domains are interpreted to be the result of ICDR. The oldest dates are 514.4 ± 3.7 Ma and the youngest are 496.5 ± 4.9 Ma. Zr concentrations in the core of the grain correspond to an apparent temperature of 965 ± 65 °C, consistent with

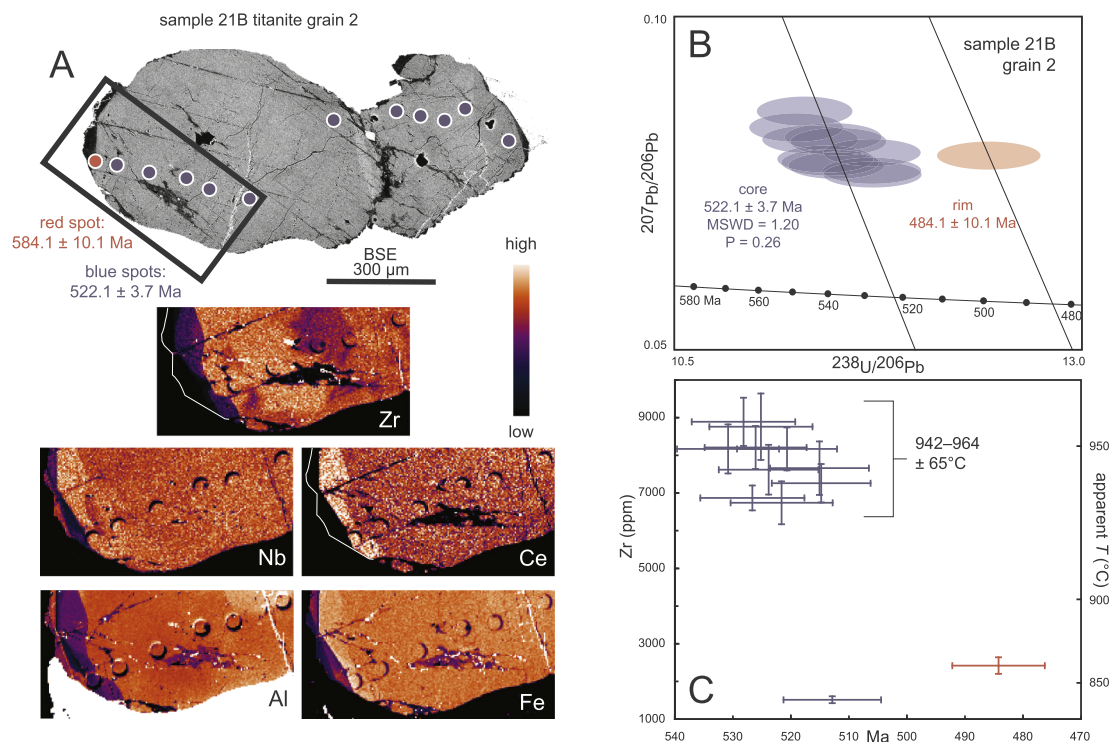


Fig. 4. Titanite data from sample 21B2 grain 2 from the Anosyen domain. (A) EPMA x-ray maps of trace elements and back-scattered-electron image of sample 21B2 titanite grain 2. The core of the grain is homogeneous in most elements, but has a diffuse, low-Zr domain near the center. The rim of the grain is characterized by three lobate compositional domains (best seen in Zr, Nb, and Al), similar to the zoning patterns observed in sample 21B2 grain 1 (Fig. 3) and is also interpreted to reflect replacement of the precursor titanite by titanite of a different composition during reaction with a fluid. (B) The unmodified core of the titanite yields a consistent date of 522 Ma; a single analysis of lobate rim domain yields a date of 484 Ma. (C) Apparent Zr temperatures from the unaltered core of the grain range from 942 to 964 °C, consistent with independent estimates of peak temperature metamorphism which occurred at ~ 550 Ma (Holder et al., 2018a). Preservation of peak- T Zr concentrations during low- T alteration (U/Th-He monazite dates of 530–510 Ma indicate $T \leq 400$ °C at this time; Montel et al., 2018), suggest that titanite-quartz-zircon equilibrium was not maintained during resetting of U-Pb dates.

independent estimates for the metamorphic peak (Boger et al., 2012; Holder et al., 2018a, 2018b; Horton et al., 2016; Jöns and Schenk, 2011). Zr concentrations in cross-cutting domains of different composition correspond to lower apparent temperatures of 850–940 °C.

The core of sample 21B2 grain 2 (Fig. 4) is homogeneous in most elements, but exhibits mottled Zr zoning. The rim of the grain is characterized by three lobate compositional domains (best seen in Zr, Nb, and Al), similar to the zoning patterns observed in sample 21B2 grain 1 (Fig. 3) and also interpreted to be the result of ICDR. The core of the titanite is 522.1 ± 3.7 Ma; a single analysis of the lobate rim domains (spot size larger than the domain widths) yielded a date of 484.1 ± 10.1 Ma. Apparent Zr temperatures from the core of the grain are 950 ± 65 °C, consistent with independent estimates of peak

metamorphic temperature (Boger et al., 2012; Holder et al., 2018a, 2018b; Horton et al., 2016; Jöns and Schenk, 2011). The diffuse, low-Zr domain in the core and the lobate rim domain yield apparent Zr temperatures of ~ 850 °C.

Data from titanite in sample 22A of the Anosyen domain are shown in Fig. 5. Back-scattered electron images show a relatively homogeneous titanite with domains of distinct composition occurring along fractures and as irregular patches in the interiors of grains, interpreted to be the result of ICDR. The alteration features do not extend along grain boundaries. Two grains were dated. Most of titanite grain 1 is 522.7 ± 4.6 Ma; an altered domain is 506.1 ± 6.7 Ma. All analyses of grain 2, from altered and unaltered titanite, are 527.7 ± 3.8 Ma. Apparent Zr temperatures from the unaltered titanite are 950 ± 65 °C,

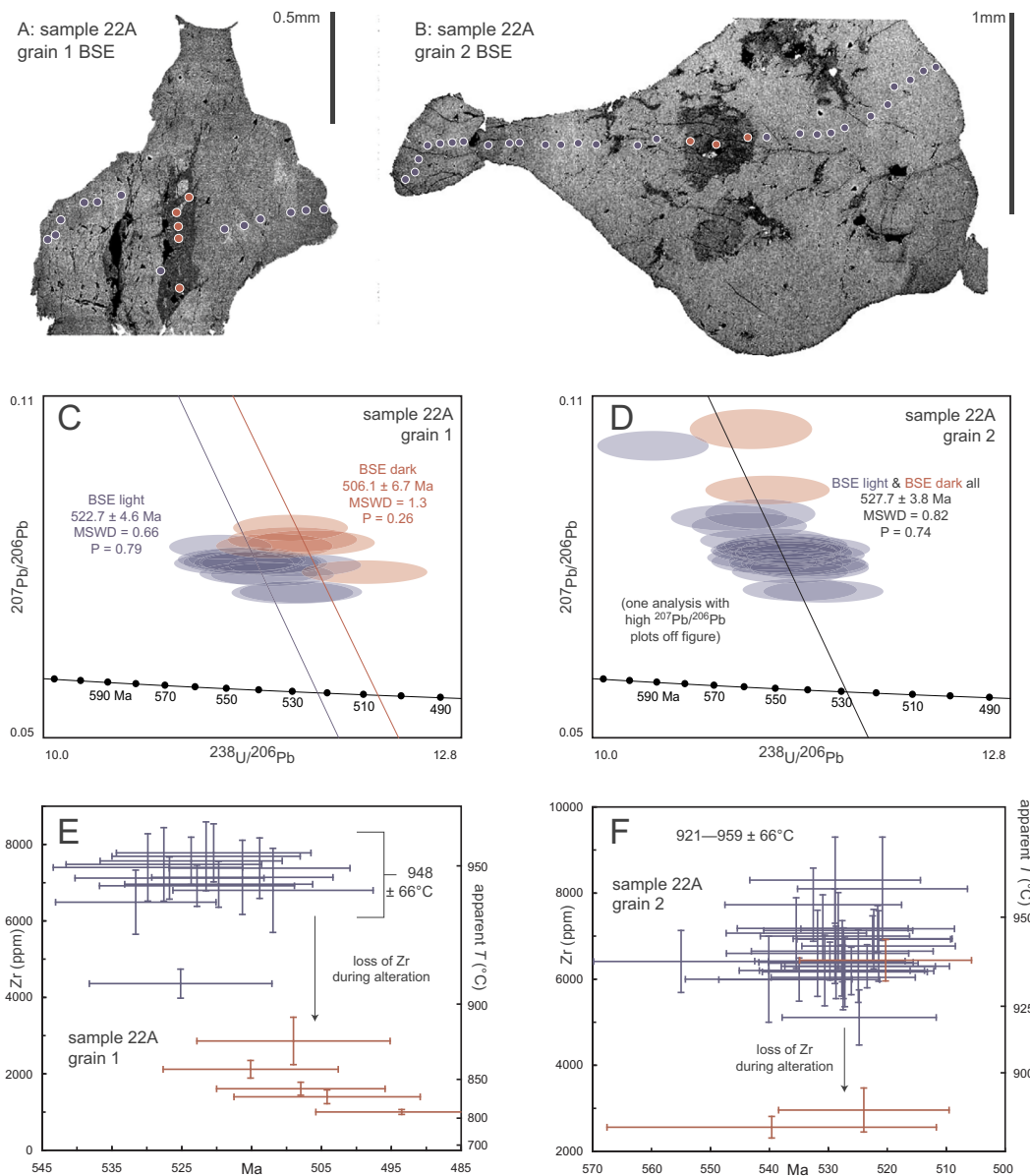


Fig. 5. Titanite data from sample 22A from the Anosyen domain. (A) Back-scattered electron image of sample 22A grain 1 showing compositional modification along fractures. (B) Back-scattered electron image of sample 22A grain 2 showing compositional modification along fractures and in isolated patches within the grain. (C) Analyses of unaltered titanite from grain 1 yielded a consistent date of 523 Ma; the altered portion of the grain yielded a consistent date of 506 Ma. (D) Analyses of altered and unaltered titanite from grain 2 yielded a consistent date of 528 Ma (in agreement with the unaltered portion of grain 1 within uncertainty). (E–F) Zr concentrations of the unaltered titanite are homogeneous, corresponding to an apparent temperature of 948 ± 66 °C, consistent with estimates of peak temperature metamorphism, which occurred at ~ 550 Ma (Holder et al., 2018a). Zr concentrations of the altered titanite are lower and heterogeneous, corresponding to apparent temperatures of 810–879 °C. Preservation of peak- T Zr concentrations during low- T alteration (U/Th–He monazite dates of 530–510 Ma indicate $T \leq 400$ °C at this time; Montel et al., 2018), suggest that titanite–quartz–zircon equilibrium was not maintained during resetting of U–Pb dates.

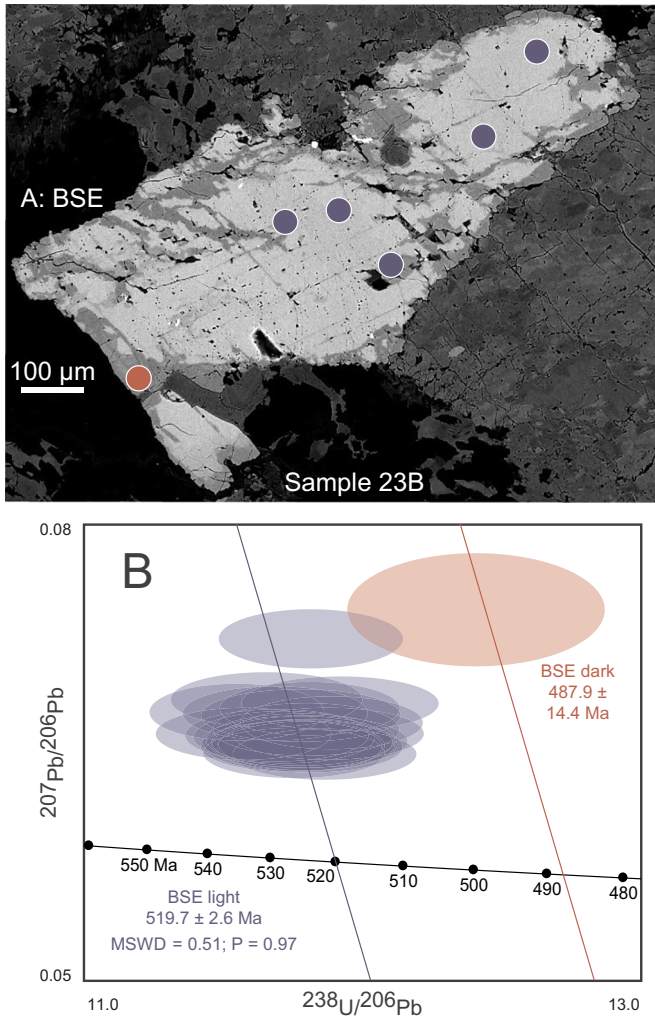


Fig. 6. Titanite data from sample 23B from the Anosyen domain. (A) Back-scattered electron image of a titanite grain showing alteration along the grain boundary and fractures. (B) U-Pb analyses from the unaltered portion of the grain (and other grains not shown) yield a consistent date of 519 Ma. A single analysis of the altered portion of the grain was 488 Ma.

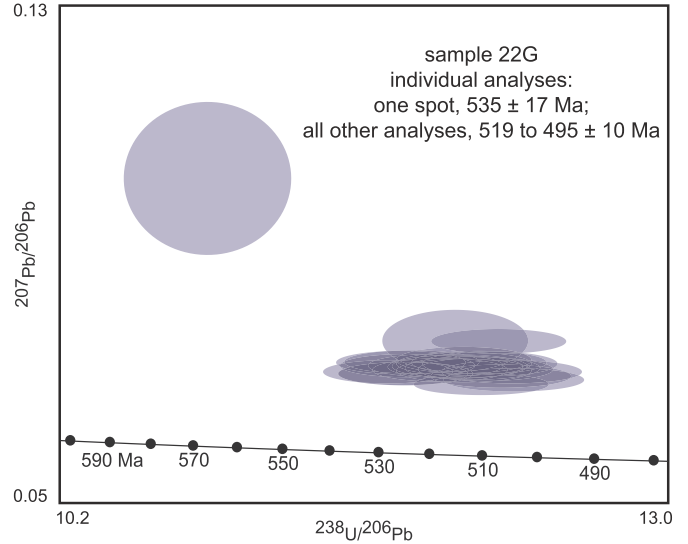


Fig. 8. Titanite data from sample 22G from the Anosyen domain. LASS spot analyses range from 519 to 495 ± 10 Ma.

consistent with independent estimates of peak metamorphic temperature (Boger et al., 2012; Holder et al., 2018a, 2018b; Horton et al., 2016; Jöns and Schenk, 2011); apparent Zr temperatures from the altered titanite are 800–900 °C.

Data from titanite in sample 23B of the Anosyen domain are shown in Fig. 6. Back-scattered electron images of a titanite grain show alteration along fractures and grain boundaries. The cores of the titanite grains is 519.7 ± 2.6 Ma; a single analysis of altered titanite near the grain rim is 488 ± 13 Ma. The apparent Zr temperature of the titanite cores is 908 ± 60 °C. The apparent Zr temperature of the altered rim is 696 ± 50 °C.

Data from titanite in sample 22D of the Anosyen domain are shown in Fig. 7. U-Pb dates range from 525 to 482 ± 11 Ma. U-Pb transects were measured in seven titanite grains. No core–rim zoning was observed in any grain. In five of the grains, all analyses are compatible with single population ages of either 507 ± 3.4 or 492.2 ± 2.6 Ma. Two titanite grains have bimodal distributions of dates corresponding to the two single-population dates identified in the other five grains. This rock does not have quartz, so no Zr temperatures are reported.

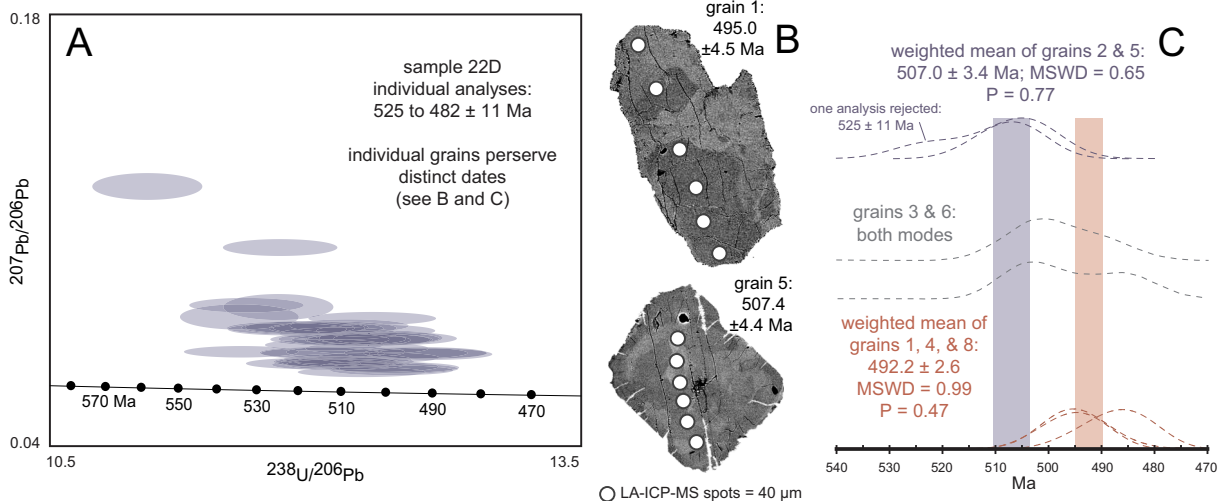


Fig. 7. Titanite data from sample 22D from the Anosyen domain. (A) LASS spot analyses range from 525 to 482 Ma. (B) Back-scattered electron images of two grains from the same thin section. All analyses from each grain yield a single date, but the dates from the two grains differ by 12 Ma (dates shown are weighted means ± 2se). (C) Probability distribution functions of all analyses of seven titanite grains from the same thin section. All the data (excluding a single older analysis) can be described as fitting one of two discrete dates: 507 or 492 Ma. Only two of seven dated grains clearly preserve both generations of dates.

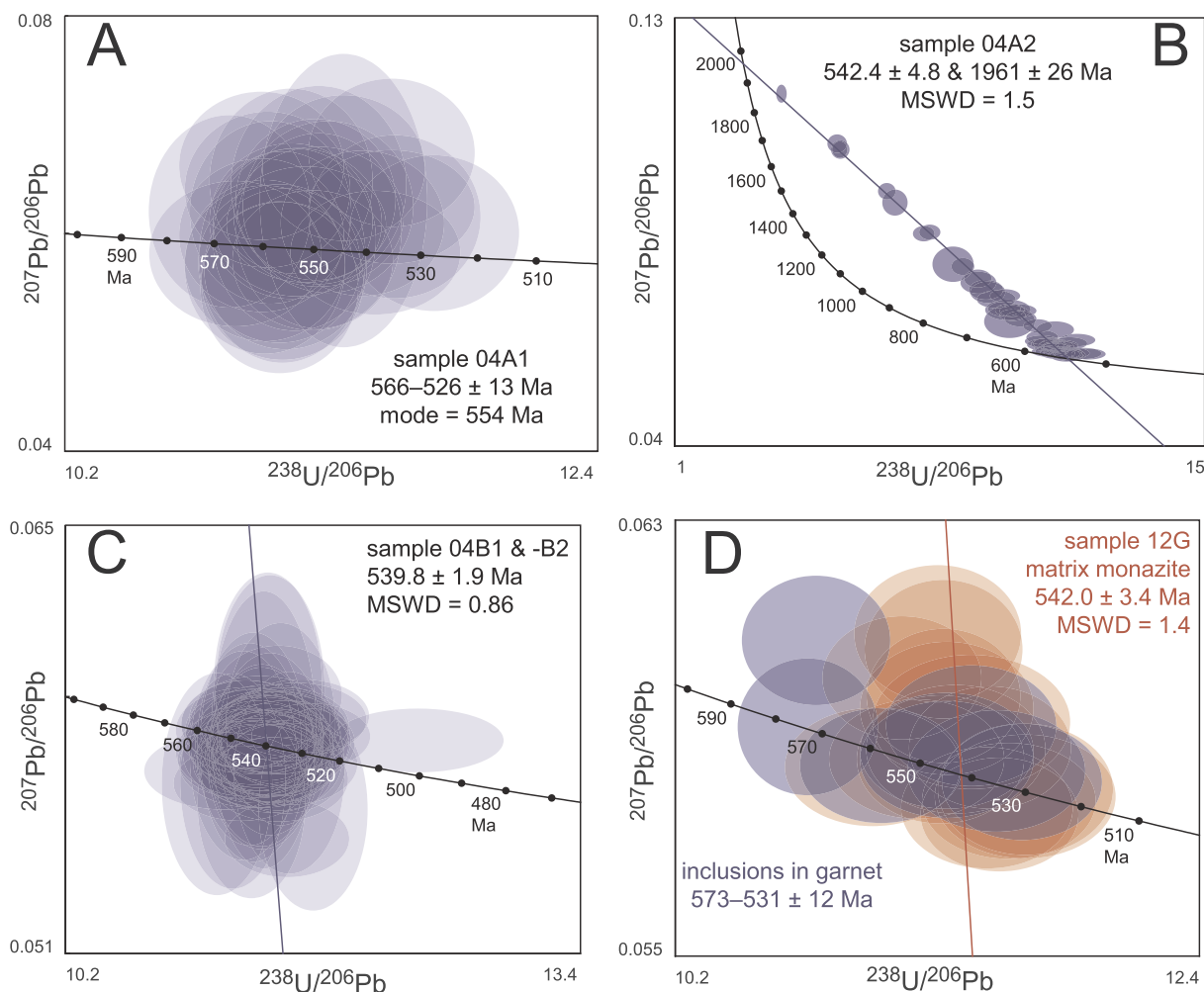


Fig. 9. Monazite U-Pb dates from felsic and pelitic gneisses in the Ikalamavony domain. (A) LASS spot analyses from sample 04A1 range from 566 to 526 ± 13 Ma. (B) All monazite dates from sample 04A2 define a discordia between 1961 ± 26 Ma and 542.4 ± 4.8 Ma. (C) All monazite dates from samples 04B1 and -B2 define a single-population age of 539.8 ± 1.9 Ma. (D) Monazite dates from the matrix of sample 12G define a single-population age of 542.0 ± 3.4 Ma. LASS spot analyses of monazite inclusions in garnet range from 573 to 531 ± 12 Ma.

Data from titanite in sample 22G are shown in Fig. 8. U-Pb dates range from 519 ± 11 to 496 ± 10 Ma. This rock does not have quartz, so no Zr temperatures are reported. In three samples—08B, 16A, and 22A4—all U-Pb analyses gave single-population dates. Concordia diagrams for these samples are shown in Fig. A.1. Dates are: 08B, 524.1 ± 2.8 Ma; 16A, 526.5 ± 2.3 Ma; sample 22A4, 521.6 ± 3.6 Ma.

4.2. Monazite petrochronology

Monazite U-Pb dates were collected from five samples from three outcrops in the Ikalamavony domain between Ankaramena and Ilosy. Concordia diagrams for these samples are shown in Fig. 9. Monazite spot dates from sample 04A1 are 566 to 526 Ma; the mode of dates is 554 Ma (as with the titanite dates, the monazite dates should be considered ± 2% accurate). Analyses from sample 04A2 define a single-population discordia between 1960 ± 26 Ma and 542 ± 5 Ma (2se of the upper and lower intercepts). Dates from samples 04B1 and 04B2 are homogeneous at 540 ± 2 Ma (weighted mean ± 2se). Dates from monazite outside of garnet in sample 12G are 542 ± 3 Ma (weighted mean ± 2se); dates from monazite inclusions in garnet range from 570 Ma to the same as the monazite outside garnet.

In aggregate, the monazite dates from the Ikalamavony domain are unimodal at 540 Ma. This mode of dates is the same as the unaltered

titanite in sample 12D2, which is interpreted to record peak-temperature conditions, consistent with the independently inferred timing of peak metamorphism for the Ikalamavony and southern Antananarivo domains (Ganne et al., 2014; Grégoire et al., 2009). Alternatively, the mode in monazite dates might be interpreted as the onset of cooling and partial melt crystallization (sample 04A is a migmatite) in which case the mode of dates is a minimum age for peak metamorphism (Stepanov et al., 2012; Yakymchuk and Brown, 2014). The older monazite dates (~570 Ma) in samples 12G (inclusions in garnet only) and 04A1 are tentatively interpreted to record earlier, prograde metamorphism (~450–600 °C for the first monazite growth at the expense of allanite in pelitic rocks; Spear, 2010). The inferred timing of prograde, peak, and retrograde metamorphism in the Ikalamavony domain proposed here are consistent with those proposed for the Anosyen domain (Holder et al., 2018a) and the correlative granulite domains of south India (Blereau et al., 2016; Johnson et al., 2015; Taylor et al., 2014).

4.3. Thermobarometry of the Ikalamavony domain

The maximum apparent Zr-in-titanite temperatures from samples in the Anosyen domain agree with the inferred conditions of peak metamorphism (900–1000 °C; Fig. 10; Boger et al., 2012; Holder et al., 2018a, 2018b; Horton et al., 2016; Jöns and Schenk, 2011). The *P-T* conditions of metamorphism in the Ikalamavony domain are less well

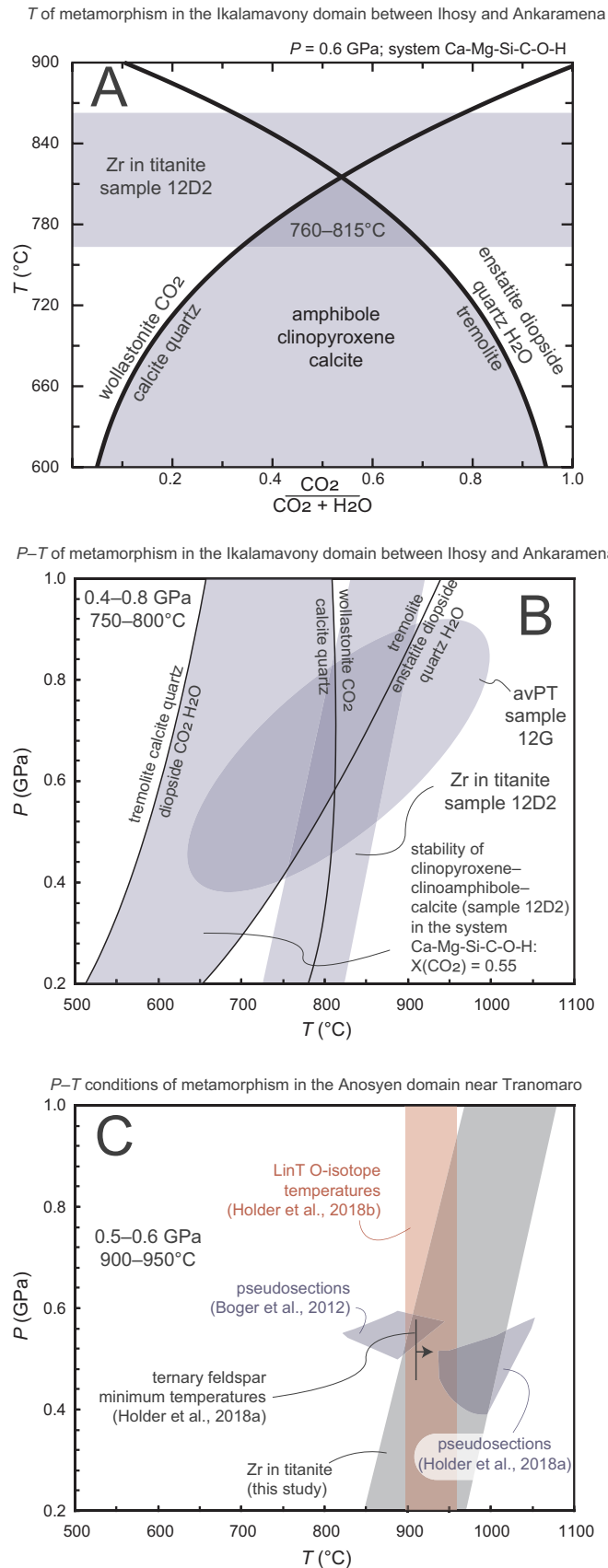


Fig. 10. Summary of P - T estimates for the rocks in this study from the Ikalamavony domain (A–B) and Anosyen domain (C). (A) The stability of calcite–quartz–Ca–amphibole and the Zr-in-titanite temperature from sample 12D2 of the Ikalamavony domain agree between 760 and 815 °C. (B) The stability of calcite–quartz–amphibole in sample 12D2 ($X_{\text{CO}_2} = \sim 0.55$, from A), the Zr-in-titanite temperature from sample 12D2, and garnet–biotite–plagioclase–sillimanite equilibria of sample 12G indicate the Ikalamavony domain between Ihosy and Ankaramena was metamorphosed at 0.4–0.8 GPa and 750–800 °C. (C) Pseudosections, O-isotope thermometry, ternary-feldspar thermometry, and Zr-in-titanite thermobarometry indicate that the Anosyen domain near Tranomaro was metamorphosed at 0.5–0.6 GPa and 900–950 °C.

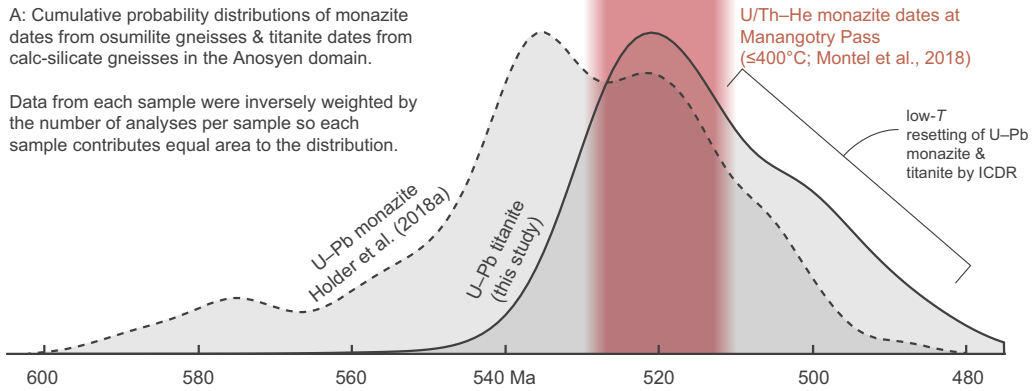
documented than those in the Anosyen domain. Based on the coexistence of Ca–amphibole, clinopyroxene, and calcite in sample 12D2, Zr-in-titanite temperatures from sample 12D2, and garnet–biotite–plagioclase–sillimanite–quartz equilibria in sample 12G, metamorphic conditions recorded in the Ikalamavony domain between Ankaramena and Ihosy are 0.4–0.8 GPa and 750–800 °C (Fig. 10). This temperature estimate is slightly higher than those estimated from pseudosections of muscovite- and relict-kyanite-bearing rocks in the Ikalamavony domain to the northwest (0.6–0.9 GPa and ~ 700 °C; GAF-BGR, 2008b), but consistent with the absence of muscovite and kyanite in the samples of this study. The P and T estimates of this study are higher than those inferred from a pseudosection of calc-silicate gneiss near Ankaramena (~ 0.4 GPa and ~ 650 °C; Ganne et al., 2014). The reason for the difference between P - T estimates of this study and those of Ganne et al. is unclear. One possible explanation is that the sample studied by Ganne et al. was collected near the faulted contact between the Ikalamavony and Antananarivo domains and might not come from the same structural level as those from this study, which were collected within the interior of the Ikalamavony domain.

5. Discussion

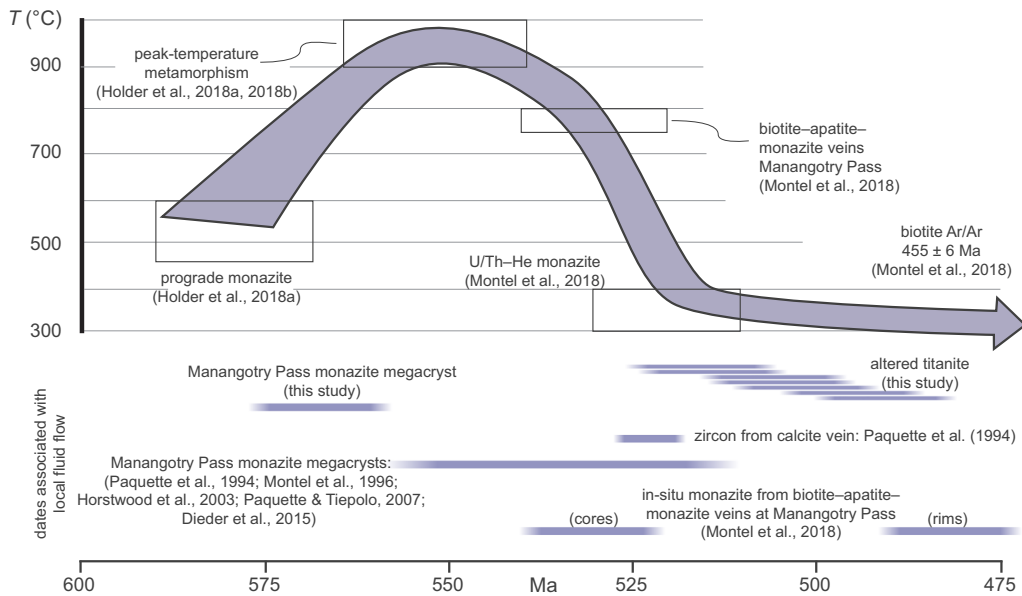
5.1. Post-UHT fluid flow in the Anosyen domain

Titanite dates from the Anosyen domain are the same or younger than U/Th–He dates from the large monazite at Manangotry Pass, within uncertainty—530 to 510 Ma, thought to represent cooling below 400 °C (Montel et al., 2018; Fig. 11)—but older than $^{40}\text{Ar}/^{39}\text{Ar}$ biotite dates (~ 300 °C; 481 ± 4 Ma in the Beraketa Shear Zone that separates the Anosyen and Androyen domains, Martin et al., 2014; 453 ± 6 Ma at Manangotry Pass, Montel et al., 2018). Based on these observations, along with pervasive lobate and patchy zoning interpreted to be the result of ICDR, and the absence of core-rim decreases in titanite U–Pb dates suggestive of diffusional Pb loss, the dates are interpreted to record resetting by 300–400 °C hydrothermal fluids. Evidence for ICDR is observed in titanite samples separated by 10's to ~ 100 km, but differences in U–Pb dates among samples—even among titanite grains in the same thin section—indicate that titanite resetting by ICDR was localized, as expected for hydrothermal activity. The highest apparent Zr-in-titanite temperatures agree with independent estimates for peak metamorphic temperatures (900–950 °C), despite U–Pb dates corresponding to 300–400 °C, suggesting that titanite–quartz–zircon equilibrium was not achieved during low-temperature ICDR or that small inclusions/exsolution of a Zr-rich phase were present and incorporated into the LA-ICP-MS analyses. Such Zr-rich inclusions/exsolution were searched for by SEM and avoided during LA-ICP-MS analysis where identified; however, nm-scale inclusions/exsolution that formed during ICDR might not have been recognized and may warrant future study by transition-electron microscopy (TEM) or atom-probe tomography (APT).

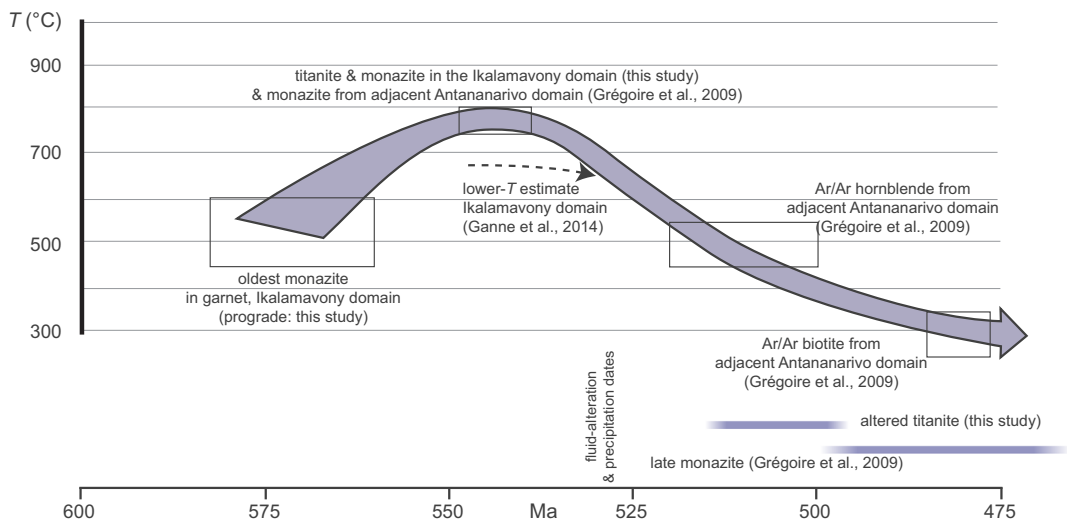
The regional metasomatism recorded by the titanite in calc-silicate gneisses between 530 and 490 Ma also appears to be recorded by monazite in the nearby osumilite-bearing pelitic gneisses studied by Holder et al. (2018a; Fig. 11). This is consistent with the findings of



B: Temperature–time path for the Anosyen domain near Tranomaro



C: Temperature–time path for the Ikalamavony and southern Antananarivo domains near Ankaramena



(caption on next page)

Fig. 11. Summary of titanite data for the Ikalamavony and Anosyen domains in relationship to other petro-/thermochronology. (A) Comparison of U-Pb titanite (this study) and monazite (Holder et al., 2018a) dates from the Anosyen domain. Both petrochronometers yielded abundant dates in agreement with or younger than U/Th–He dates (Montel et al., 2018). Both chronometers are inferred to have been reset at low temperature by interface-coupled dissolution-precipitation reactions. Similar interpretations have been made for monazite from the Trivandrum block of south India (Taylor et al., 2014; Blereau et al., 2016), which is inferred to have been contiguous with the Anosyen domain during metamorphism. (B) Temperature–time path of the Anosyen domain after Holder et al. (2018a) showing the abundance of radiometric dates specifically tied to focused fluid flow during retrogression of the terrane, including the titanite dates of this study. (C) Temperature–time path for the Ikalamavony domain from monazite and titanite petrochronology (this study) and nearest available $^{40}\text{Ar}/^{39}\text{Ar}$ thermochronology from the adjacent Antananarivo domain (Grégoire et al., 2009).

Taylor et al. (2014) and Blereau et al. (2016), who inferred widespread resetting of monazite by post-metamorphic fluid influx in the Trivandrum block of south India, inferred to have been contiguous with the Anosyen domain during the Ediacaran–Cambrian orogeny. Taylor et al. (2014) and Blereau et al. (2016) inferred that the monazite-altering fluids in India were aqueous brines, whereas some of the fluid inclusions in calc-silicates of Madagascar are pure CO_2 (Rakotondrazafy et al., 1996). Both aqueous-brine and CO_2 -rich fluid inclusions are common in granulites (e.g. Touret and Huizenga, 2011). Because the titanite dates suggest fluid-flow was localized, it is hypothesized that the composition of metasomatizing fluid was spatially and/or temporally variable and likely influenced by local rock composition (see Pili et al., 1997a, 1997b, for discussion of possible fluid sources). For more information on the regional variability and complexity of metasomatism in southern Madagascar, see Boulvais et al., 1998, 2000; Martin et al., 2014; Moine et al., 1998; Pili et al., 1997a, 1997b; Rakotondrazafy et al., 1996; and Ramambazafy et al., 1998.

5.2. Thermal history of the Ikalamavony domain and geological significance of titanite petrochronology in sample 12D2

U-Pb titanite dates from unaltered titanite in sample 12D2 of the Ikalamavony domain are the same as the mode of U-Pb monazite dates from nearby pelitic gneisses. Based on the absence of core–rim zoning in U-Pb titanite dates, and Zr-in-titanite temperatures that are the same or higher than other estimates for peak metamorphism within the domain (see above), these dates (537.2 ± 2.6 Ma [2se], ± 11 Ma [2% accuracy]) are interpreted to record titanite growth at or close to the time of peak metamorphism in the Ikalamavony domain, in agreement with the thermal history proposed by Ganne et al. (2014) and Grégoire et al. (2009) for the Ikalamavony and Antananarivo domains near Ankaramena. The P – T conditions at this time are estimated to have been 0.4–0.8 GPa and 750–800 °C (Fig. 10). Prograde metamorphism is inferred to have begun ~570 Ma (same as in the Anosyen domain [Holder et al., 2018a] and in its correlative, the Trivandrum domain of south India [Blereau et al., 2016; Johnson et al., 2015; Taylor et al., 2014]) based on the oldest U-Pb monazite dates from sample 04A1 and dates from monazite inclusions in garnet in sample 12G.

U-Pb titanite dates from altered titanite in sample 12D2 are 504.0 ± 2.6 Ma [2se; ± 10 Ma, 2% accuracy], 32.3 ± 3.6 Myr younger than the inferred timing of peak metamorphism. The dates from altered titanite are equivalent to a nearby $^{40}\text{Ar}/^{39}\text{Ar}$ amphibole date and older than a nearby $^{40}\text{Ar}/^{39}\text{Ar}$ biotite date (Grégoire et al., 2009) suggesting $300 < T_{\text{alteration}} \leq 500$ °C. The homogeneity of U-Pb dates from the altered titanite suggests that ICDR is an efficient mechanism for resetting the U-Pb system in titanite. Unlike the U-Pb dates, the Zr concentrations are heterogeneous in the altered domains. Zr-in-titanite temperatures are less than or equal to the metamorphic peak (750–800 °C; Figs. 2,10) but greater than the inferred alteration temperature ($300 < T_{\text{alteration}} \leq 500$ °C) inferred from nearby thermochronology. This is interpreted to indicate that titanite–quartz–zircon equilibrium was not achieved during alteration. Zr was lost from the titanite during alteration, but the apparent temperatures are not indicative of the temperature at which the U-Pb dates were reset. This

may be due to non-penetrative fluid flow; alteration of the titanite occurred only along fractures through the titanite grain, but not along grain boundaries (Fig. 2), possibly prohibiting equilibration between titanite and the other phases in the rock. Alternatively, nm-scale Zr-rich inclusions/exsolution too small for identification during BSE imaging might have been present and may warrant future study by TEM or APT.

6. Conclusions

This study builds upon the growing body of evidence that fluid-mediated replacement reactions are one of the primary mechanisms by which U-Pb dates are reset in petrochronometers (see Engi, 2017, for review of phosphates; Rubatto, 2017, for review of zircon). In southern Madagascar:

- 1) Regionally extensive, but non-penetrative fluid flow (dates differ among samples and among grains within individual samples) between 530 and 490 Ma was the primary mechanism by which U-Pb titanite dates were reset following granulite-facies metamorphism.
- 2) Resetting of U-Pb titanite dates was apparently efficient (dates from individual altered domains are homogeneous) and occurred at temperatures as low as 300–400 °C.
- 3) Apparent Zr temperatures (temperatures calculated assuming titanite–quartz–zircon equilibrium) in altered titanite are less than or equal to the metamorphic peak, but higher than the inferred alteration temperature, suggesting that Zr was removed, but titanite–quartz–zircon equilibrium was not achieved during alteration. Future nm-scale investigation might be useful to discern whether the higher-than-expected Zr concentrations are hosted in the titanite lattice or in nm-scale exsolved inclusions that formed during ICDR.

Lobate, discontinuous domains of distinct chemical composition with $< \mu\text{m}$ -scale boundaries—interpreted in this study to be indicative of ICDR—are a common feature of metamorphic titanite (Bonamici et al., 2015; Castelli and Rubatto, 2002; Franz and Spear, 1985; Garber et al., 2017; Kohn, 2017; Marsh and Smye, 2017; Rubatto and Hermann, 2001; Spencer et al., 2013; Walters and Kohn, 2017). It is hypothesized that fluid–titanite interaction, not volume diffusion, is the primary mechanism by which titanite dates are reset at $T < 850$ °C (Gao et al., 2012; Garber et al., 2017; Kohn, 2017; Kohn and Corrie, 2011; Marsh and Smye, 2017; Spencer et al., 2013; Stearns et al., 2015, 2016; Walters and Kohn, 2017).

Supplementary data to this article can be found online at <https://doi.org/10.1016/j.chemgeo.2018.11.017>.

Acknowledgements

A. Kylander-Clark and G. Seward assisted with data collection. Preliminary interpretations of the data were discussed with A. Kylander-Clark, G. Seward, and J. Garber. R. Taylor and F. Corfu are thanked for constructive reviews. B. Kamber is thanked for constructive comments and editorial handling. Funding: This work was supported by the University of California, Santa Barbara and the National Science Foundation [grant number NSF-EAR-1348003].

References

- Aleinikoff, J.N., Wintsch, R.P., Tollo, R.P., Unruh, D.M., Fanning, C.M., Schmitz, M.D., 2007. Ages and origins of rocks of the Killingworth dome, south-central Connecticut: Implications for the tectonic evolution of southern New England. *Am. J. Sci.* 307, 63–118. <https://doi.org/10.2475/01.2007.04>.
- Blereau, E., Clark, C., Taylor, R.J.M., Johnson, T.E., Fitzsimons, I.C.W., Santosh, M., 2016. Constraints on the timing and conditions of high-grade metamorphism, charnockite formation, and fluid-rock interaction in the Trivandrum Block, southern India. *J. Metamorph. Geol.* 34, 527–549. <https://doi.org/10.1111/jmg.12192>.
- Boger, S.D., White, R.W., Schulte, B., 2012. The importance of iron speciation ($\text{Fe}^{+2}/\text{Fe}^{+3}$) in determining mineral assemblages: an example from the high-grade aluminous metapelites of southeastern Madagascar. *J. Metamorph. Geol.* 30, 997–1018. <https://doi.org/10.1111/jmg.12001>.
- Bonamico, C.E., Fanning, C.M., Kozdon, R., Fournelle, J.H., Valley, J.W., 2015. Combined oxygen-isotope and U–Pb zoning studies of titanite: new criteria for age preservation. *Chem. Geol.* 398, 70–84. <https://doi.org/10.1016/j.chemgeo.2015.02.002>.
- Boulvais, P., Fourcade, S., Gruau, G., Moine, B., Cuney, M., 1998. Persistence of pre-metamorphic C and O isotopic signatures in marbles subject to Pan-African granulite-facies metamorphism and U–Th mineralization (Tranomaro, Southeast Madagascar). *Chem. Geol.* 150, 247–262. [https://doi.org/10.1016/S0009-2541\(98\)00062-X](https://doi.org/10.1016/S0009-2541(98)00062-X).
- Boulvais, P., Fourcade, S., Moine, B., Gruau, G., Cuney, M., 2000. Rare-earth elements distribution in granulite-facies marbles: a witness of fluid-rock interaction. *Lithos* 53, 117–126. [https://doi.org/10.1016/S0024-4937\(00\)00013-X](https://doi.org/10.1016/S0024-4937(00)00013-X).
- Castelli, D., Rubatto, D., 2002. Stability of Al- and F-rich titanite in metacarbonate: Petrologic and isotopic constraints from a polymetamorphic eclogitic marble of the internal Sesia zone (Western Alps). *Contrib. Mineral. Petrol.* 142, 627–639. <https://doi.org/10.1007/s00410-001-0317-6>.
- Chambers, J.A., Kohn, M.J., 2012. Titanium in muscovite, biotite, and hornblende: Modeling, thermometry, and rutile activities of metapelites and amphibolites. *Am. Mineral.* 97, 543–555. <https://doi.org/10.2138/am.2012.3890>.
- Cherniak, D.J., 1993. Lead diffusion in titanite and preliminary results on the effects of radiation damage on Pb transport. *Chem. Geol.* 110, 177–194. [https://doi.org/10.1016/0009-2541\(93\)90253-F](https://doi.org/10.1016/0009-2541(93)90253-F).
- Corfu, F., 1996. Multistage zircon and titanite growth and inheritance in an Archean gneiss complex, Winnipeg River Subprovince, Ontario. *Earth Planet. Sci. Lett.* 141, 175–186. [https://doi.org/10.1016/0012-821X\(96\)00064-7](https://doi.org/10.1016/0012-821X(96)00064-7).
- Corfu, F., Muir, T.L., 1989. The Hemlo-Heron Bay greenstone belt and Hemlo Au–Mo deposit, Superior Province, Ontario, Canada: 2. Timing of metamorphism, alteration and Au mineralization from titanite, rutile, and monazite U–Pb geochronology. *Chem. Geol. Isot. Geosci. Sect.* 79, 201–223.
- Donovan, J.J., Singer, J.W., Armstrong, J.T., 2016. A new EPMA method for fast trace element analysis in simple matrices. *Am. Mineral.* 101, 1839–1853. <https://doi.org/10.2138/am-2016-5628>.
- Engi, M., 2017. Petrochronology based on REE-minerals: monazite, allanite, xenotime, apatite. *Rev. Mineral. Geochem.* 83, 365 LP–418. <https://doi.org/10.2138/rmg.2017.83.12>.
- Franz, G., Spear, F.S., 1985. Aluminous titanite (sphene) from the Eclogite Zone, south-central Tauern Window, Austria. *Chem. Geol.* 50, 33–46. [https://doi.org/10.1016/0009-2541\(85\)90110-X](https://doi.org/10.1016/0009-2541(85)90110-X).
- Frost, B.R., Chamberlain, K.R., Schumacher, J.C., 2000. Sphene (titanite): phase relations and role as a geochronometer. *Chem. Geol.* 172, 131–148. [https://doi.org/10.1016/S0009-2541\(00\)00240-0](https://doi.org/10.1016/S0009-2541(00)00240-0).
- GAF-BGR, 2008a. Explanatory Notes for the Anosyen Domain, Southeast Madagascar. Ministère de L'énergie et des Mines (MEM/SG/DG/UCP/PGRM), Antananarivo, Republique de Madagascar.
- GAF-BGR, 2008b. Explanatory notes for the Itremo-Ikalamavony Domain, Central and Western Madagascar Réalisation des Travaux de Cartographie Géologique de Madagascar, Révision Approfondie de la Cartographie Géologique et Minière Aux 1–89.
- Ganne, J., Nédélec, A., Grégoire, V., Gouy, S., de Parseval, P., 2014. Tracking Late-Pan-African fluid composition evolution in the ductile crust of Madagascar: insight from phase relation modelling of retrogressed gneisses (province of Fianarantsoa). *J. Afr. Earth Sci.* 94, 100–110. <https://doi.org/10.1016/j.jafrearsci.2013.10.004>.
- Gao, X.-Y., Zheng, Y.-F., Chen, Y.-X., Guo, J., 2012. Geochemical and U–Pb age constraints on the occurrence of polygenetic titanites in UHP metagranite in the Dabie orogen. *Lithos* 136–139, 93–108. <https://doi.org/10.1016/j.lithos.2011.03.020>.
- Garber, J.M., Hacker, B.R., Kylander-Clark, A.R.C., Stearns, M.A., Seward, G., 2017. Controls on trace element uptake in metamorphic titanite: implications for petrochronology. *J. Petrol.* 58, 1031–1057. <https://doi.org/10.1093/petrology/egx046>.
- Gehrels, G.E., Valencia, V.A., Ruiz, J., 2008. Enhanced precision, accuracy, efficiency, and spatial resolution of U–Pb ages by laser ablation-multicollector-inductively coupled plasma-mass spectrometry. *Geochem. Geophys. Geosyst.* 9, 1–13. <https://doi.org/10.1029/2007GC001805>.
- Ghent, E.D., Stout, M.Z., 1984. TiO_2 activity in metamorphosed pelitic and basic rocks: principles and applications to metamorphism in southeastern Canadian Cordillera. *Contrib. Mineral. Petrol.* 86, 248–255. <https://doi.org/10.1007/BF00373670>.
- Grégoire, V., Nédélec, A., Monié, P., Montel, J.-M., Ganne, J., Ralison, B., 2009. Structural reworking and heat transfer related to the late-Pan-African Angavo shear zone of Madagascar. *Tectonophysics* 477, 197–216. <https://doi.org/10.1016/j.tecto.2009.03.009>.
- Hayden, L.A., Watson, E.B., Wark, D.A., 2008. A thermobarometer for sphene (titanite). *Contrib. Mineral. Petrol.* 155, 529–540. <https://doi.org/10.1007/s00410-007-0256-y>.
- Holder, R.M., Hacker, B.R., Horton, F., Rakotondrazafy, A.F.M., 2018a. Ultrahigh-temperature osumilite gneisses in southern Madagascar record combined heat advection and high rates of radiogenic heat production in a long-lived high-T orogen. *J. Metamorph. Geol.* 36, 855–880. <https://doi.org/10.1111/jmg.12316>.
- Holder, R.M., Sharp, Z.D., Hacker, B.R., 2018b. LinT, a simplified approach to oxygen-isotope thermometry and speedometry of high-grade rocks: an example from ultrahigh-temperature gneisses of southern Madagascar. *Geology*. <https://doi.org/10.1130/G40207.1>.
- Holland, T.J.B., Powell, R., 2011. An improved and extended internally consistent thermodynamic dataset for phases of petrological interest, involving a new equation of state for solids. *J. Metamorph. Geol.* 29, 333–383. <https://doi.org/10.1111/j.1525-1314.2010.00923.x>.
- Horton, F., Hacker, B.R., Kylander-Clark, A.R.C., Holder, R.M., Jöns, N., 2016. Focused radiogenic heating of middle crust caused ultrahigh temperatures in southern Madagascar. *Tectonics* 35, 293–314. <https://doi.org/10.1002/2015TC004040>.
- Johnson, T.E., Clark, C., Taylor, R.J.M., Santosh, M., Collins, A.S., 2015. Prograde and retrograde growth of monazite in migmatites: an example from the Nagercoil Block, southern India. *Geosci. Front.* 6, 373–387. <https://doi.org/10.1016/j.gsf.2014.12.003>.
- Jöns, N., Schenk, V., 2011. The ultrahigh temperature granulites of southern Madagascar in a polymetamorphic context: implications for the amalgamation of the Gondwana supercontinent. *Eur. J. Mineral.* 23, 127–156. <https://doi.org/10.1127/0935-1221/2011/0023-2087>.
- Kirkland, C.L., Fougereuse, D., Reddy, S.M., Hollis, J., Saxey, D.W., 2018. Assessing the mechanisms of common Pb incorporation into titanite. *Chem. Geol.* 483, 558–566. <https://doi.org/10.1016/j.chemgeo.2018.03.026>.
- Kirkland, C.L., Hollis, J., Danišik, M., Petersen, J., Evans, N.J., McDonald, B.J., 2017. Apatite and titanite from the Karrat Group, Greenland; implications for charting the thermal evolution of crust from the U–Pb geochronology of common Pb bearing phases. *Precambrian Res.* 300, 107–120. <https://doi.org/10.1016/j.precamres.2017.07.033>.
- Kohn, M.J., 2017. Titanite Petrochronology. *Rev. Mineral. Geochem.* 83. <https://doi.org/10.2138/rmg.2017.83.13>.
- Kohn, M.J., Corrie, S.L., 2011. Preserved Zr-temperatures and U–Pb ages in high-grade metamorphic titanite: evidence for a static hot channel in the Himalayan orogen. *Earth Planet. Sci. Lett.* 311, 136–143. <https://doi.org/10.1016/j.epsl.2011.09.008>.
- Kretz, R., 1983. Symbols for rock-forming minerals. *Am. Mineral.* 68, 277–279.
- Kylander-Clark, A.R.C., 2017. Petrochronology by laser-ablation inductively coupled plasma mass spectrometry. *Rev. Mineral. Geochem.* 83, 183–196. <https://doi.org/10.2138/rmg.2017.83.6>.
- Kylander-Clark, A.R.C., Hacker, B.R., Cottle, J.M., 2013. Laser-ablation split-stream ICP petrochronology. *Chem. Geol.* 345, 99–112. <https://doi.org/10.1016/j.chemgeo.2013.02.019>.
- Kylander-Clark, A.R.C., Hacker, B.R., Mattinson, J.M., 2008. Slow exhumation of UHP terranes: titanite and rutile ages of the Western Gneiss Region, Norway. *Earth Planet. Sci. Lett.* 272, 531–540. <https://doi.org/10.1016/j.epsl.2008.05.019>.
- Marsh, J.H., Smye, A.J., 2017. U–Pb systematics and trace element characteristics in titanite from a high-pressure mafic granulite. *Chem. Geol.* 466, 403–416. <https://doi.org/10.1016/j.chemgeo.2017.06.029>.
- Martin, R.F., Randrianandrisana, A., Boulvais, P., 2014. Ampandrandava and similar phlogopite deposits in southern Madagascar: derivation from a silicocarbonatic melt of crustal origin. *J. Afr. Earth Sci.* 94, 111–118. <https://doi.org/10.1016/j.jafrearsci.2013.08.002>.
- Mezger, K., Rawnsley, C.M., Bohlen, S.R., Hanson, G.N., 1991. U–Pb garnet, sphene, monazite, and rutile ages: implications for the duration of high-grade metamorphism and cooling histories, Adirondack Mts., New York. *J. Geol.* 99, 415–428. <https://doi.org/10.1086/629503>.
- Moine, B., Ramambazafy, A., Rakotondrazafy, M., Ravolomianinarivo, B., Cuney, M., de Parseval, P., Antananarivo, M., 1998. The role of fluor-rich fluids in the formation of the thorianite and sapphire deposits from SE Madagascar. *Mineral. Mag.* 62, 999–1000.
- Montel, J.-M., Razafimahatratra, D., de Parseval, P., Poitrasson, F., Moine, B., Seydoux-Guillaume, A.-M., Pik, R., Arnaud, N., Gibert, F., 2018. The giant monazite crystals from Manangotry (Madagascar). *Chem. Geol.* 484, 36–50. <https://doi.org/10.1016/j.chemgeo.2017.10.034>.
- Paton, C., Hellstrom, J., Paul, B., Woodhead, J., Hergt, J., 2011. Iolite: freeware for the visualisation and processing of mass spectrometric data. *J. Anal. At. Spectrom.* 26, 2508. <https://doi.org/10.1039/c1ja10172b>.
- Pili, É., Ricard, Y., Lardeaux, J.-M., Sheppard, S.M.F., 1997a. Lithospheric shear zones and mantle-crust connections. *Tectonophysics* 280, 15–29. [https://doi.org/10.1016/S0040-1951\(97\)00142-X](https://doi.org/10.1016/S0040-1951(97)00142-X).
- Pili, É., Sheppard, S.M.F., Lardeaux, J.-M., Martelat, J.-E., Nicollet, C., 1997b. Fluid flow vs. scale of shear zones in the lower continental crust and the granulite paradox. *Geology* 25, 15–18. [https://doi.org/10.1130/0091-7613\(1997\)025<0015:FFVSOS>2.3.CO;2](https://doi.org/10.1130/0091-7613(1997)025<0015:FFVSOS>2.3.CO;2).
- Powell, R., Holland, T., 1994. Optimal geothermometry and geobarometry. *Am. Mineral.* 79, 120–133.
- Putnis, A., 2009. Mineral replacement reactions. *Rev. Mineral. Geochem.* 70, 87–124. <https://doi.org/10.2138/rmg.2009.70.3>.
- Rakotondrazafy, A.F.M., Moine, B., Cuney, M., 1996. Mode of formation of hibonite (CaAl₁₂O₁₉) within the U–Th skarns from the granulites of S-E Madagascar. *Contrib. Mineral. Petrol.* 123, 190–201. <https://doi.org/10.1007/s004100050150>.
- Ramambazafy, A., Moine, B., Rakotondrazafy, M., Cuney, M., 1998. Signification des fluides carboniques dans les granulites et les skarns du Sud-Est de Madagascar in the granulites and skarns of southeast. *Géomatériaux* 327, 743–748.
- Rapa, G., Groppo, C., Rolfo, F., Petrelli, M., Mosca, P., Perugini, D., 2017. Titanite-bearing calc-silicate rocks constrain timing, duration and magnitude of metamorphic CO₂

- degassing in the Himalayan belt. *Lithos* 292–293, 364–378. <https://doi.org/10.1016/j.lithos.2017.09.024>.
- Romer, R.L., Rötzler, J., 2003. Effect of metamorphic reaction history on the U-Pb dating of titanite. *Geol. Soc. Lond. Spec. Publ.* 220, 147–158. <https://doi.org/10.1144/GSL.SP.2003.220.01.08>.
- Rubatto, D., 2017. Zircon: the metamorphic mineral. *Rev. Mineral. Geochem.* 83, 261–295. <https://doi.org/10.2138/rmg.2017.83.10>.
- Rubatto, D., Hermann, J., 2001. Exhumation as fast as subduction? *Geology* 29, 3–6. [https://doi.org/10.1130/0091-7613\(2001\)029<0003:EAFAS>?2.0.CO](https://doi.org/10.1130/0091-7613(2001)029<0003:EAFAS>?2.0.CO).
- Spandler, C., Hermann, J., Rubatto, D., 2004. Exsolution of thortveitite, yttrialite, and xenotime during low-temperature recrystallization of zircon from New Caledonia, and their significance for trace element incorporation in zircon. *Am. Mineral.* 89, 1795–1806. <https://doi.org/10.2138/am-2004-11-1226>.
- Spear, F.S., 2010. Monazite-allanite phase relations in metapelites. *Chem. Geol.* 279, 55–62. <https://doi.org/10.1016/j.chemgeo.2010.10.004>.
- Spear, F.S., Parrish, R.R., 1996. Petrology and cooling rates of the Valhalla Complex, British Columbia, Canada. *J. Petrol.* 37, 733–765.
- Spencer, K.J., Hacker, B.R., Kylander-Clark, A.R.C., Andersen, T.B., Cottle, J.M., Stearns, M.A., Poletti, J.E., Seward, G.G.E., 2013. Campaign-style titanite U–Pb dating by laser-ablation ICP: Implications for crustal flow, phase transformations and titanite closure. *Chem. Geol.* 341, 84–101. <https://doi.org/10.1016/j.chemgeo.2012.11.012>.
- Stearns, M.A., Cottle, J.M., Hacker, B.R., Kylander-Clark, A.R.C., 2016. Extracting thermal histories from the near-rim zoning in titanite using coupled U-Pb and trace-element depth profiles by single-shot laser-ablation split stream (SS-LASS) ICP-MS. *Chem. Geol.* 422, 13–24. <https://doi.org/10.1016/j.chemgeo.2015.12.011>.
- Stearns, M.A., Hacker, B.R., Ratschbacher, L., Rutte, D., Kylander-Clark, A.R.C., 2015. Titanite petrochronology of the Pamir gneiss domes: Implications for middle to deep crust exhumation and titanite closure to Pb and Zr diffusion. *Tectonics* 34, 784–802. <https://doi.org/10.1002/2014TC003774>.
- Stepanov, A.S., Hermann, J., Rubatto, D., Rapp, R.P., 2012. Experimental study of monazite/melt partitioning with implications for the REE, Th and U geochemistry of crustal rocks. *Chem. Geol.* 300–301, 200–220. <https://doi.org/10.1016/j.chemgeo.2012.01.007>.
- Taylor, R.J.M., Clark, C., Fitzsimons, I.C.W., Santosh, M., Hand, M., Evans, N., McDonald, B., 2014. Post-peak, fluid-mediated modification of granulite facies zircon and monazite in the Trivandrum Block, southern India. *Contrib. Mineral. Petrol.* 168, 1–17. <https://doi.org/10.1007/s00410-014-1044-0>.
- Touret, J.L.R., Huizenga, J.-M., 2011. Fluids in granulites. In: *Geological Society of America Memoirs*, pp. 25–37. [https://doi.org/10.1130/2011.1207\(03\)](https://doi.org/10.1130/2011.1207(03)).
- Tucker, R.D., Råheim, A., Krogh, T.E., Corfu, F., 1987. Uranium-lead zircon and titanite ages from the northern portion of the Western Gneiss Region, south-central Norway. *Earth Planet. Sci. Lett.* 81, 203–211. [https://doi.org/10.1016/0012-821X\(87\)90156-7](https://doi.org/10.1016/0012-821X(87)90156-7).
- Walters, J.B., Kohn, M.J., 2017. Protracted thrusting followed by late rapid cooling of the Greater Himalayan Sequence, Annapurna Himalaya, Central Nepal: Insights from titanite petrochronology. *J. Metamorph. Geol.* 35, 897–917. <https://doi.org/10.1111/jmg.12260>.
- Wendt, I., Carl, C., 1991. The statistical distribution of the mean squared weighted deviation. *Chem. Geol. Isot. Geosci. Sect.* 86, 275–285. [https://doi.org/10.1016/0168-9622\(91\)90010-T](https://doi.org/10.1016/0168-9622(91)90010-T).
- Yakymchuk, C., Brown, M., 2014. Behaviour of zircon and monazite during crustal melting. *J. Geol. Soc. Lond.* 171, 465–479. <https://doi.org/10.1144/jgs2013-115>.